Journal of Nuclear Materials 385 (2009) 334–338

Contents lists available at ScienceDirect

Journal of Nuclear Materials

journal homepage: www.elsevier.com/locate/jnucmat

Positron annihilation study of neutron irradiated model alloys and of a reactor pressure vessel steel

M. Lambrecht [a,b,*], A. Almazouzi [a]

[a] SCK•CEN, Nuclear Materials Sciences Institute, Boeretang 200, B-2400 Mol, Belgium
[b] University of Ghent, Department of Materials Science and Engineering, Technologiepark 903, B-9052 Gent, Belgium

ARTICLE INFO

PACS:
28.52.Fa
62.20.−x
78.70.Bj

ABSTRACT

The hardening and embrittlement of reactor pressure vessel steels are of great concern in the actual nuclear power plant life assessment. This embrittlement is caused by irradiation-induced damage, and positron annihilation spectroscopy has been shown to be a suitable method for analysing most of these defects. In this paper, this technique (both positron annihilation lifetime spectroscopy and coincidence Doppler broadening) has been used to investigate neutron irradiated model alloys, with increasing chemical complexity and a reactor pressure vessel steel. It is found that the clustering of copper takes place at the very early stages of irradiation using coincidence Doppler broadening, when this element is present in the alloy. On the other hand, considerations based on positron annihilation spectroscopy analyses suggest that the main objects causing hardening are most probably self-interstitial clusters decorated with manganese in Cu-free alloys. In low-Cu reactor pressure vessel steels and in (Fe, Mn, Ni, Cu) alloys, the main effect is still due to Cu-rich precipitates at low doses, but the role of manganese-related features becomes pre-dominant at high doses.

1. Introduction

The irradiation-induced hardening and embrittlement of reactor pressure vessel (RPV) steels are of great concern for nuclear power plant (NPP) life assessment. For the sake of their preservation, NPPs have already been subjected to a lot of investigations [1]. It was observed that the materials used for the reactor vessels are prone to embrittle due to irradiation. However, the real nature of the radiation damage responsible for this embrittlement, and its evolution with dose still require close examination.

Irradiation-induced embrittlement in RPV steels is conventionally ascribed to three main causes [2]: precipitation, matrix damage and grain boundary segregation. While precipitation and segregation have been profoundly studied [2], it is still unclear, what the nature and the main mechanisms of the formation of matrix damage are. Small vacancy and interstitial clusters are well-known to be produced directly in displacement cascades [3,4]. These clusters aggregate to larger defects such as nano-voids and self-interstitial loops. At the same time, solute atoms may diffuse to these clusters, giving rise to large, complex defect-solute configurations. But which solutes and how and why they stabilize clusters is still a debated matter.

For this present work, the experiments conducted by positron annihilation spectroscopy (PAS) in the European framework PERFECT were used to interpret the corresponding hardening results that were obtained by tensile tests. PAS gives valuable information on irradiation-induced vacancy type defects [5–8]. In this technique, the positron is applied as a probe. As anti-particle of the electron, the positron is trapped by defects with a different electron density than the bulk-material, such as vacancies, vacancy clusters, interfaces, second phase particles, dislocations, etc. [9]. Moreover, due to the difference in positron affinity of the different atoms, positrons can annihilate with higher probability in the precipitates as compared to the bulk-material [10]. The power of PAS lies in its 'self-seeking' and non-destructive nature, which gives the possibility to find very small defects (>0.1 nm) even in very low concentrations (>1 ppm).

Significant progress in the characterization of vacancy clusters has been made by PAS during the past decades [11–15]. The focus is now being put on the chemical surroundings of the clusters that are sensitive to positrons, to obtain a better understanding of the nature of the matrix damage. Positrons are indeed sensitive to the precipitates. Therefore, a substantial effort is being re-deployed to use this technique to identify the ultimate causes of hardening and embrittlement in RPV steels. In this paper, the results obtained from PAS investigations of different neutron irradiated Fe and (Fe, Cu) alloys as well as of (Fe, Mn, Ni) and (Fe, Mn, Ni, Cu) alloys, are described and discussed. The results are then correlated to the

* Corresponding author. Address: SCK•CEN, Nuclear Materials Sciences Institute, Boeretang 200, B-2400 Mol, Belgium. Tel.: +32 14 33 30 13; fax: +32 14 32 12 16.
E-mail address: Marlies.Lambrecht@SCKCEN.BE (M. Lambrecht).

0022-3115/$ - see front matter © 2008 Elsevier B.V. All rights reserved.
doi:10.1016/j.jnucmat.2008.12.020

irradiation-induced hardening data obtained in the same samples [16]. For the sake of comparison, also a Western type RPV steel was examined.

2. Materials and irradiation conditions

Starting from electrolytic iron, seven different model alloys were fabricated, with growing chemical complexity between two extremes, i.e. pure Fe, (Fe, C), (Fe, 0.1% Cu), (Fe, 0.3% Cu), (Fe, Mn, Ni), (Fe, Mn, Ni, Cu) and a real RPV steel. The materials were prepared using argon-arc melting and zone refinement methods. The resulting ingots were cold-worked after austenisation tempering. A final heat treatment at 1075 K for 1 h was performed to release the stresses and to get well re-crystallized materials. This was followed by water quenching. Table 1 provides the composition of the alloys.

All the materials have been irradiated in the test reactor BR2 at SCK•CEN, to different doses. The temperature and the pressure were maintained constant during irradiation between 565 and 570 K and at 150 bar, respectively. In a previous paper [17], the entire set of specimens irradiated up to 0.1 dpa (i.e. about 40 years of radiation and the theoretical end-of-life of the NPPs) is taken into consideration. In this present paper these results are compared to the ones of the samples irradiated with a damage of 0.2 displacements per atom (dpa) ($\sim 13 \times 10^{19}$ cm^{-2} for the considered neutron flux of $(9.5 \pm 0.5) \times 10^{13}$ cm^{-2} s^{-1}, with $E_n > 1$ MeV), with the aim to reveal the effect of each chemical element on the development of matrix damage and its influence on the material hardening at higher irradiation doses.

3. Measurement and analysis

Positron annihilation lifetime spectroscopy (PALS) and coincidence Doppler broadening (CDB) spectroscopy, both available in the hot cell laboratory of SCK•CEN, have been used in a complementary way. PALS measurements give information on the electron density of the material at the place of annihilation, while CDB spectroscopy allows measuring the momentum distribution of the electron–positron annihilated pair, giving information of the chemical environment of the annihilation site. These results have been correlated with the mechanical properties that were obtained from tensile tests, measured before and after irradiation.

3.1. Tensile test measurements

The mechanical properties of the samples were determined, by performing tensile tests. The specimens used for these measurements had a gauge length of 15 mm with a diameter of 3 mm. The heads of the specimens had a diameter of 8 mm and the total length was 26 mm. All measurements were performed at room temperature, with a strain rate of about 2×10^{-4} s^{-1}.

Starting from the engineering stress–strain curves, the yield strength was calculated. Further on in this paper, the increase of yield strength in the irradiated material, compared to the non-irradiated one, is used as reference property. In the case of the non-irradiated (Fe, Mn, Ni, Cu) alloy, due to a shortage of material, only hardness measurements could be performed. From these data it was however possible to estimate reliably the corresponding yield strength value, based on obtained correlations.

Table 1
The composition of the studied alloys.

Material	Concentration (wt%)			
	C	Cu	Mn	Ni
Pure Fe	<0.002	<0.005	0.010	<0.005
(Fe, C)	0.005	0.015	0.015	<0.005
(Fe, 0.1% Cu)	<0.002	0.11	0.007	<0.005
(Fe, 0.3% Cu)	<0.002	0.315	0.010	<0.005
(Fe, Mn, Ni)	<0.002	<0.005	1.09	0.75
(Fe, Cu, Mn, Ni)	<0.002	0.105	1.08	0.72
French RPV steel	0.14	0.064	1.30	0.75

3.2. Positron lifetime measurements

Non- and irradiated specimens of $10 \times 10 \times 1$ mm^3 have been first surface-polished to a mirror finish, and then chemically etched using a ($HF + H_2O_2 + H_2O$) solution to remove the deformed surface layer. The specimens, taken two-by-two in a sandwich-like fashion, with the positron source in-between, were mounted in the positron specimen holder under biologically shielded environment. The sandwich was then automatically loaded in the measurement cell between three BaF_2 detectors working in anti-coincidence mode. All measurements were performed at room temperature using a ^{22}Na positron source, with a strength of 2 MBq, wrapped in Kapton foils.

Within a few picoseconds after the positron is implanted in the material by its source, a γ-ray is emitted with an energy of 1274 keV. This γ-ray is detected and used as the birth signal. The positron will thermalize in the material ($\sim$100 μm during a few ps) and diffuse ($\sim$100 nm) until it is trapped by a defect. At this defect, the positron will stay until it annihilates with an electron. During annihilation, the electron–positron pair will disappear by emitting two anti-collinear γ-rays with an energy of 511 keV. The lifetime of the positron can thus be measured as the time delay between the birth and the annihilation gammas.

As the studied specimens were neutron irradiated, the standard technique had to be adapted. Depending on the radioactivity of the samples, the distance separating the detectors was adjusted to minimise the background. Care was taken to separate correctly the γ-peaks coming from the specimens and those related to the positrons, by following the procedure described by Jardin et al. [18]. Due to their activation, the acquisition of statistically relevant number of counts, namely at least one million, has required up to 1 month for these high dose irradiated samples. The analysis of the obtained spectra has been performed using the LT-software [19]. The resolution of the setup was constantly checked to be about 175 ps, while the source contribution was set to 15% with a single lifetime of 393 ps. The lifetime spectra have been decomposed into two lifetimes, the shortest τ_1 and the longest one τ_2 with their respective intensities I_1 and I_2 (with $I_1 + I_2 = 1$). The main lifetime used within this paper has been measured, but it is very close to the calculated value ($\tau_m = I_1 \times \tau_1 + I_2 \times \tau_2$). More detailed information about the experimental setup is given by Jardin et al. [18,20]. Here, it has been shown that for our setup, the lifetime measured in non-irradiated pure Fe samples corresponds to (107.57 ± 0.38) ps.

3.3. Coincidence Doppler broadening measurements

The momentum of the annihilating positron–electron pair is transmitted to the annihilation quanta. The longitudinal component p_L of this momentum along the direction of the γ-ray emission produces a Doppler shift $\Delta E = p_L c/2$ on the energy of the annihilation radiation (c is the speed of light). This shift results in a broadening of the annihilation peak at 511 keV ($=mc^2$; m is the mass of an electron), which is easily observed in an accurate energy measurement of the photons.

The specimens for CDB have been prepared in the same way as for PALS. The CDB measurements have been performed as described by Verheyen et al. [16]. The analysis of the results have been made using CDB ratio curves, obtained by normalizing the

momentum distribution to the one of unirradiated defect-free pure Fe. The *S*- and *W*-parameters were extracted from each spectrum. They are defined, respectively as the ratio of low-momentum ($|p_L| < 2.5 \times 10^{-3}\, mc$) and high-momentum ($15 \times 10^{-3}\, mc < |p_L| < 25 \times 10^{-3}\, mc$) regions in the CDB spectrum to the total region.

As the total curves are normalized, the *S*- and *W*-parameters will be correlated. Nevertheless, both parameters will contain different information. The valence electrons can only give rise to a small difference in the energy of the annihilation γ-rays, while the core electrons can lead to all different kinds of energy changes. The former will thus contribute to the peak of the CDB curves, and will therefore be observed by the *S*-parameter. The latter, on the other hand, will contribute to the wide momentum region. Therefore, the *W*-parameter qualifies these electrons. Moreover, the changes in the γ-energies due to the core electrons will possess specific information of the chemical elements.

4. Results and discussions

In the previous paper [17], it was shown that most of the hardening in Cu containing alloys is due to precipitates, which are produced already at the start of the irradiation [21]. A minor influence of the matrix damage was also observed at 0.1 dpa. There was predicted that the contribution due to the matrix damage would become more pronounced at higher irradiation doses. At the same time, two possible matrix damage features were introduced, i.e. manganese decorated self-interstitial atom (SIA) loops and vacancy (v)-induced precipitates consisting mainly of manganese and nickel. The farmer was believed to be the most important, although no real prove was given. In this paper the matrix damage will be further discussed, using the results at higher dose.

Here, the results of the yield strength, the CDB measurements and the PALS results of the samples irradiated at 0.1 dpa are repeated in Figs. 1–3, respectively. The results of the yield strength, as well as those for the CDB measurements are expressed as the *increase* with respect to the non-irradiated values (the CDB spectra have first been normalized to pure iron). For the PALS results, no such *increase* has been defined. As the results for non-irradiated, defect-free samples only have one component, such a definition would not be appropriate. Therefore, it should be mentioned that the results for the non-irradiated materials are all very close to the value of defect-free pure iron, i.e. 107 ps.

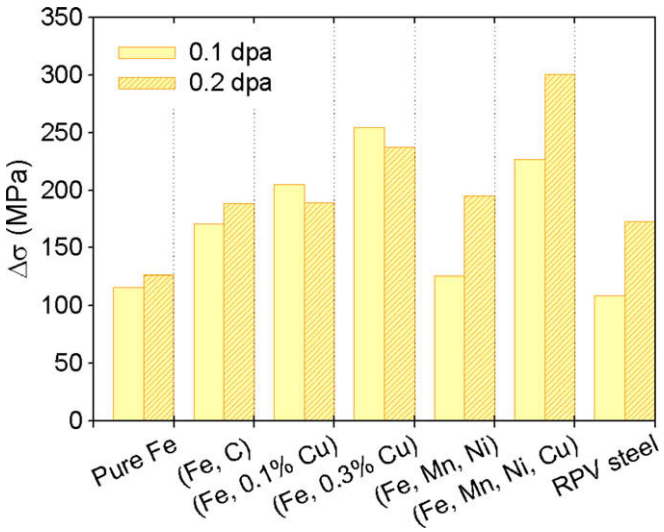

Fig. 1. Comparison of the hardening (change of yield strength of the irradiated sample compared to the unirradiated one) for all materials. The values are given for the materials irradiated up to 0.1 and 0.2 dpa.

The results of the samples irradiated at 0.2 dpa are shown in the same figures for comparison. While for the hardening, the biggest changes have been seen in the alloys containing manganese and nickel (including the RPV steel), almost no changes have been found in the positron results for these alloys. By PAS, drastic changes only have been observed for the binary (Fe, Cu) alloys.

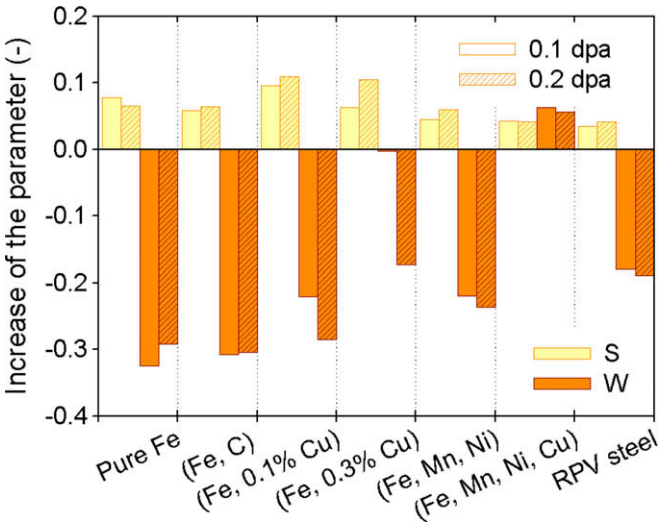

Fig. 2. The low (*S*-parameter) and high (*W*-parameter) momentum fractions of the CDB spectra are shown for all materials. The *increase* of the parameter is given as the difference between the value for the irradiated specimen and the one for the non-irradiated specimen of the same material. The values are given for the materials irradiated up to 0.1 and 0.2 dpa.

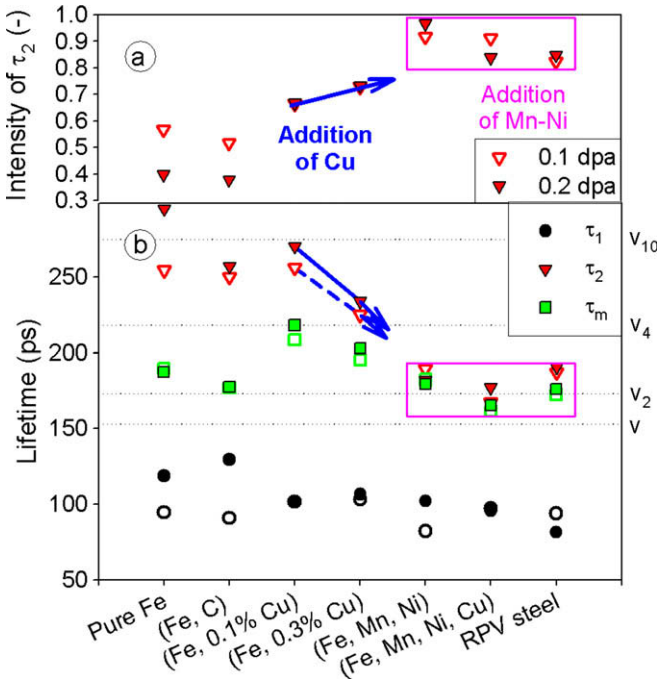

Fig. 3. Comparison of the positron lifetime results for all materials. The results are divided into two lifetime components (τ_1 and τ_2) and their average is given as well (τ_m). In part (a), the intensity (I_2) of τ_2 is given (with $I_1(\tau_1) + I_2(\tau_2) = 1$), while in part (b), the results for τ_1, τ_2 and τ_m are shown. The values are given for the materials irradiated up to 0.1 and 0.2 dpa. The theoretical values of positron lifetime in v-clusters obtained by Kuriplach et al. [22] are also reported.

It has been observed for all the materials that vacancy clusters were produced under irradiation, as a second PALS component (i.e. a component related to the defects) occurs. These vacancy clusters seem to grow drastically in pure iron during further irradiation. As the number density of the second PALS component decreases considerably, this growth, observed by the second component itself, is mainly caused by agglomeration of smaller defects. The mean lifetime, on the other hand, does not change when the irradiation dose increases. This indicates that most of the newly produced vacancies disappear at sinks, although some single vacancies, that are located too far from the sinks to disappear, are present in the matrix as well. These vacancies have a lifetime, which is much smaller than the one of the clusters and therefore they will be found as a part of the first PALS component. An increase of this first component is thus observed. The obvious decrease of number of defects causes a small return of the CDB results to the initial, defect-free state, because fewer positrons will be trapped by the remaining defects.

The same observations are found for the (Fe, C) alloy; the main lifetime stays constant, while both the first and second component increases when the dose increases. There should be noticed that the presence of carbon restricts the vacancy growth, while more single vacancies are present in the matrix at the high dose compared to pure iron. C thus reduces the mobility of the vacancies at this high dose.

In both alloys the hardening increases a little. In [17], it was explained that most of the hardening in these alloys is due to SIA loops, as the contribution of the vacancy clusters is negligible. Also the fact that the hardening increase in-between the two investigated irradiation doses is more explicit for the alloy containing carbon impurities, indicate that the vacancy clusters play only a minor role in the hardening, as the ones found in pure iron were observed to be bigger.

In both binary (Fe, Cu) alloys a small decrease of the hardening is observed. This was not expected, as no decrease of the hardening was found before. It is found in literature that copper plays a role on the hardening in the very early stage of irradiation, but saturates quite rapidly [2,23]. More detailed investigations should thus be performed to determine the origin of this decrease. In this paper, this has been done using the PAS results.

In Fig. 4 the full CDB curves are shown for the (Fe, Cu) alloy containing 0.3% of copper, normalized to pure iron. It is clear that for both irradiation doses, the copper-specific peak is still present.

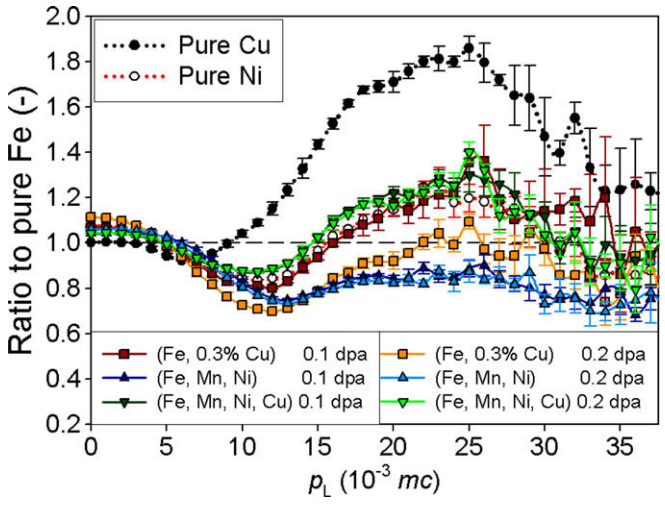

Fig. 4. The low full CDB spectra (normalized to pure iron) are shown for (Fe, 0.3% Cu), (Fe, Mn, Ni) and (Fe, Mn, Ni, Cu) at 0.1 and 0.2 dpa. The spectra of pure copper and nickel are added as well, for comparison.

Therefore, it is possible to conclude that copper is still located at the annihilation, and that the precipitates are not dissolved. The same has been found for the alloy containing 0.1% of copper. Although the *W*-parameter of the CDB measurements decreases enormously for the highest dose, it did not yet reach the value for pure irradiated iron. Also only for these alloys, a marked change of the mean lifetime is observed. More vacancies are thus observed by the PAS techniques at the highest irradiation dose compared to the lower one. As vacancies are preferentially localized in the copper-rich precipitates (see [17,24]), there can be assume that these precipitates will grow in amount of vacancies with augmenting dose, inducing an enormous decrease of *W* (positrons annihilate with valence electrons of the copper atoms), and an increase of *S* and the second PALS component. The amount of precipitates stays approximately constant, as the intensity of the second PALS component does not change for neither of the alloys.

This change of the microstructural composition of the precipitates may be the cause of the decrease in the hardening, observed by the tensile tests. Indeed, the changing amount of vacancies will lead to a changing strength of the precipitates. As the defects become softer the total hardening of the sample will decrease.

A drastic change of the hardening at the highest irradiation dose is observed for the samples containing manganese and nickel. This increase is found although no important clustering of the vacancy type of defects occurs, as it is shown by the low τ_2 values. Indeed, for the (Fe, Mn, Ni) alloy even the contrary is found; more and smaller vacancy defects are observed. This is seen by a higher intensity of a lower second PALS component, as well as by a higher *S*-value. Fig. 4 indicates that even at the highest irradiation dose, some copper and/or nickel is located at the annihilation sites. As the peak for pure nickel looks very much like the one of copper, it is impossible to distinguish which of the two elements is present. In contrast to the finding that only very small vacancy clusters are produced, a lowering of *W* for irradiation to the higher dose is found. This points to the fact that most of the new vacancies will not be combined with copper or nickel.

When also copper is added to the alloy, a little bit of clustering of vacancies is observed, what points to the presence of copper. Vacancies will gather in the copper precipitates, at the same time as they will be scattered in the matrix, combined with the other alloying elements. There can thus be assumed that no clustering of manganese and nickel occur as a result of their motion combined with vacancies.

This eliminates the hardening contribution of one of the matrix damage features ((v)-induced precipitates consisting mainly of manganese and nickel) as they have been discussed in [17]. The explanation of manganese decorated SIA loops, on the other hand, is still valid. As these loops are initiated at a lower dose, the newly produced interstitials will be trapped by them, inducing an enormous growth of the SIA loops, while the small loops are stabilized by the presence of manganese. The vacancy-solute combinations, on the other hand, are mobile. So, when they meet such a manganese-stabilized SIA loop, the vacancy can recombine with a SIA from the loop, while the solute (i.e. manganese, nickel or copper) would stay in this case and decorate the loop.

All the results in Figs. 1–3 of the RPV steel are comparable with those of the model alloys containing manganese and nickel. The results of the steel is always in-between the two model alloys.

5. Conclusions

The results of the experiments conducted for this study were used to interpret the corresponding hardening results. It was observed that most of the irradiation-induced hardening in RPV steels and their model alloys irradiated up to a damage density of 0.1 dpa

was still due to copper precipitation. But even at this irradiation dose, matrix damage already played an important role. As copper precipitation was fully completed by this dose, the influence of matrix damage becomes more manifest when the material is irradiated up to a higher dose.

It was shown that further irradiation of the binary (Fe, Cu) alloys leads to a decrease of the hardening. An increasing amount of vacancies in the copper precipitates implies a little bit of softening of these precipitates.

But for the addition of manganese and nickel to the alloys, a drastic increase of the hardening is observed. As no vacancy clustering is visible, this phenomenon is not due to manganese and/or nickel precipitation in the same way as the copper precipitated before. Therefore this hardening will be due to the appearance of manganese decorated SIA loops.

Acknowledgements

This work is partly financed by the European Union in the framework of the PERFECT Project, under contract FI60-CT-2003-5088-40.

References

[1] S.B. Fisher, J.E. Harbottle, N. Aldridge, Phil. Trans. R. Soc. Lond. A 315 (1985) 301.
[2] W.J. Phythian, C.A. English, J. Nucl. Mater. 205 (1993) 162.
[3] L. Malerba, J. Nucl. Mater. 351 (2006) 28.
[4] D. Terentyev, C. Lagerstedt, P. Olssen, K. Nordlund, J. Wallenius, C.S. Becquart, L. Malerba, J. Nucl. Mater. 351 (2006) 65.
[5] Y. Nagai, M. Hasegawa, Z. Tang, A. Hempel, K. Yubuta, T. Shimamura, Y. Kawazou, A. Kawai, F. Kano, Phys. Rev. B 61 (2000) 6574.
[6] Y. Nagai, Z. Tang, M. Hasegawa, T. Kanai, M. Saneyasu, Phys. Rev. B 63 (2001) 134110.
[7] P. Asoka-Kumar, B.D. Wirth, P.A. Sterne, R.H. Howell, G.R. Odette, Philos. Mag. Lett. 82 (2002) 609.
[8] K. Fujii, K. Fukuya, N. Nakata, K. Hono, Y. Nagai, M. Hasegawa, J. Nucl. Mater. 340 (2005) 247.
[9] M. Eldrup, B.N. Singh, J. Nucl. Mater. 251 (1997) 132.
[10] M.J. Puska, R.M. Nieminen, Rev. Mod. Phys. 66 (1994) 841.
[11] J.T. Buswell, J.P. Highton, CEGB, Berkeley Nuclear Laboratories, TPRD/B/0787/R86, 1986.
[12] G.H. Dai, P. Moser, J.C. Van Duysen, in: Proceedings of the IXth International Conference on Positron Annihilation, Szombathely (Hungary), 1991, p. 941.
[13] R.G. Carter, T. Onchi, N. Soneda, K. Dohi, J.M. Hyde, C.A. English, M.T. Hutchings, W. Server, J.F. Coste, J.C. Van Duysen, in: Proceedings of the IVth International Symposium on the Contribution of Materials Investigation to the Resolution of Problems Encountered in Pressurized Water Reactors, Fontevraud (France), 1998, p. 89.
[14] M. Valo, R. Krause, K. Saarinen, P. Hautojarvi, J.R. Hawthorne, in: R.E. Stoiler, A.S. Kumar, D.S. Gelles (Eds.), Effects of Radiation on Materials: 15th International Symposium, ASTM 1125, ASTM, Philadelphia (USA), 1992, p. 172.
[15] M. Eldrup, B.N. Singh, J. Nucl. Mater. 323 (2003) 346.
[16] K. Verheyen, M. Jardin, A. Almazouzi, J. Nucl. Mater. 351 (2006) 209.
[17] M. Lambrecht, L. Malerba, A. Almazouzi, J. Nucl. Mater. in press, Available online doi:10.1016/j.jnucmat.2008.06.030.
[18] M. Jardin, M. Lambrecht, A.A. Rempel, Y. Nagai, E. van Walle, A. Almazouzi, Nucl. Instrum. and Meth. A 568 (2006) 716.
[19] J. Kansy, Nucl. Instrum. and Meth. A 374 (1996) 235.
[20] M. Jardin, A. Almazouzi, M. Lambrecht, A.A. Rempel, Y. Nagai, E. van Walle, Phys. Stat. Sol. (c) 4 (2007) 4001.
[21] M. Lambrecht, M. Jardin, A. Almazouzi, Phys. Stat. Sol. (c) 4 (2007) 3477.
[22] J. Kuriplach, O. Melikhova, C. Domain, C.S. Becquart, D. Kulikov, L. Malerba, M. Hou, A. Almazouzi, C.A. Duque, A.L. Morales, Appl. Surf. Sci. 252 (2006) 3303.
[23] R. Chaouadi, R. Gérard, J. Nucl. Mater. 345 (2005) 65.
[24] E. Vincent, C.S. Becquart, C. Domain, J. Nucl. Mater. 351 (2006) 88.